Simulation of ASIRAS Altimeter Echoes for Snow-Covered First-Year Sea Ice

Marko P. Mäkynen, *Member, IEEE*, and Martti T. Hallikainen, *Fellow, IEEE*

***Abstract*—We have developed a simulator for the European Space Agency's Airborne SAR/Interferometric Radar Altimeter System (ASIRAS) altimeter echoes from snow-covered first-year sea ice. The simulated echoes are used to investigate how measurements are affected by the snow and ice characteristics. Our simulations show that when the snow cover is dry, the echo from the upper ice surface typically dominates. The simulated echoes prove to be very sensitive to the presence of liquid water in snow and the small-scale roughness of the ice surface. The accurate estimation of the ice freeboard is likely possible only under dry snow conditions and when the snow load is known. The ASIRAS simulator concept can also be used for the CryoSat altimeter.**

***Index Terms*—CryoSat, radar altimetry, sea ice.**

I. Introduction

THE AIRBORNE SAR/Interferometric Radar Altimeter System (ASIRAS) of the European Space Agency (ESA) was designed to support the CryoSat satellite mission, whose aim is to accurately determine the trends in sea ice and continental ice fields [1], [2]. Within the CryoSat cal/val activities, the CryoVex 2005 campaign was carried out in the Bay of Bothnia in March 2005. In this campaign, ASIRAS was operated in low-altitude mode (LAM) with the altitude varying from 300 to 1100 m. The LAM allowed simultaneous measurements with a 3-D Airborne Laser Scanner (ALS) instrument which provides cross-track scans of sea ice surface topography [3]. ASIRAS level 1B data are used to classify altimeter echoes according to various ice types and to evaluate the estimation of the ice freeboard.

An ASIRAS simulator has been programmed in Matlab for studying the behavior of the ASIRAS echoes from snow-covered Baltic Sea level and deformed ice (DI). The simulation of the ASIRAS echoes is based on the results in [2] and [4]. The simulator allows studying the contribution of snow and sea ice surface and volume echoes to the total echo, and the effect of various snow and sea ice parameters. Pending publication on all ASIRAS technical data, certain assumptions regarding the antenna and synthetic beam patterns have been made. By using the ASIRAS simulator, normalized simulated and measured echoes can be compared, and the results are used for the development of range retracking algorithms, which are the basis for the ice freeboard estimation.

Manuscript received September 25, 2008; revised January 7, 2009. First published April 24, 2009; current version published July 4, 2009.

M. P. Mäkynen is with the Finnish Meteorological Institute, 00101 Helsinki, Finland (e-mail: marko.makynen@fmi.fi).

M. T. Hallikainen is with the Department of Radio Science and Engineering, Helsinki University of Technology, 02015 Espoo, Finland (e-mail: martti.hallikainen@tkk.fi).

Digital Object Identifier 10.1109/LGRS.2009.2015968

TABLE I
SOME CHARACTERISTICS OF THE ASIRAS LAM [1], [7]–[9]

Parameter	Value
Center frequency f_0	13.5 GHz
Bandwidth B	1 GHz
Transmitted peak power P_T	5 W
Pulse repetition interval T_I	1/3000 s
Range resolution ΔR	11 cm
3 dB antenna beamwidth	9.7° along track 2.2° across track
Angular resolution of the beams ξ_b	0.904°
Aircraft altitude H	300, 500, 700 or 1100 m
Mean number of beams in the multi-looked echo	76 at 300 m 280 at 1100 m
Beam look angle θ_b	0° to 5.1°

Recently, the simulation of Ku-band altimeter echoes from sea ice has been studied in [5] and [6]. In [5], a radiative transfer model is used to simulate the variability of sea ice effective scattering surface as a function of snow depth and density. The depth of the effective scattering surface forms the basis for the ice-thickness estimation, and the results show that the snow cover has a significant impact on the estimated ice thickness. However, this model does not account for antenna gain or pulse shape effects. In [6], a simulator is developed that calculates D2P radar (Delay/Doppler Phase-monopulse Radar Altimeter) echoes using a triangular surface facet model constructed from laser elevation data, where the facet power response is described by a simple exponential function. The antenna gain and synthetic beam parameters are included in the D2P simulator, and the difference between measured and simulated echoes is used to estimate snow thickness.

II. ASIRAS Altimeter

ASIRAS uses the synthetic aperture radar technique to enhance the spatial resolution of the radar in the flight path direction [1]. Some characteristics of the ASIRAS LAM are shown in Table I. In the LAM, ASIRAS transmits a burst of $N = 32$ pulses with a pulse repetition interval T_I [7], and the return echoes are processed to 32 equally spaced beams. A number of beams from different bursts are steered to the same location on the ground and then slant-range corrected (i.e., time differences between beams with different look angles are compensated for) and finally summed together to form a multilooked echo. During the multilooking, a weighting function may be applied

1545-598X/$25.00 © 2009 IEEE

Authorized licensed use limited to: Danmarks Tekniske Informationscenter. Downloaded on November 25, 2009 at 07:27 from IEEE Xplore. Restrictions apply.

across the beams such that the central beams are more heavily weighted than those near the edges. The number of beams in the multilooked echo is a function of aircraft elevation (H) and speed (V), aperture length, and wavelength (λ_0)—the value varies and is stored in the ASIRAS data product [8]. The angular resolution of the beams is (same as the beam separation angle) [2], [7]

$$\xi_b = \frac{\lambda_0}{2NVT_I}. \tag{1}$$

The ASIRAS beam gain function is assumed here to be [2], [7]

$$d(x) = D_0 \left| \frac{\sin(N\Delta k_0 x}{N \sin(\Delta k_0 x)} \right|^2 \tag{2}$$

where D_0 is the maximum beam gain, $x = \sin\gamma\cos\lambda - \theta_b$, γ and λ are the polar and azimuthal angles measured with respect to the antenna boresight, and θ_b is the beam look angle. The along-track sampling interval Δ and the polar angle γ (i.e., the incidence angle) are

$$\Delta = VT_I \tag{3}$$

$$\gamma \approx \sqrt{c_0\tau/H} \tag{4}$$

where $\tau = t - 2H/c_0$ and t is the two-way time to the surface. It is assumed that the steered beams for a multilooked echo come from the consecutive bursts, and thus, the beam look angles are

$$\theta_b = \tan^{-1}\left(\frac{(i-1)(N\cdot\Delta)}{H}\right), \qquad i = 1, \ldots, N/2. \tag{5}$$

The beams forward and backward of the flight track are assumed to have equal beam look angles. The slant-range correction is obtained from the zero value of the beam gain function argument x

$$\tau_{\rm sl} = \frac{H}{c_0}\theta_b^2. \tag{6}$$

The system impulse response can be approximated with the sinc function [7]

$$p(t) = |\mathrm{sinc}(t/s_p)|^2 \tag{7}$$

where $s_p = t_{\rm 3dB}/0.886$ and $t_{\rm 3dB}$ is the 3-dB time width of the impulse response. An equation for the range resolution is given in [8].

An equation for the ASIRAS antenna pattern has not yet been published; the values of the maximum gain and 3-dB beamwidths are given in [9]. Here, the antenna pattern is assumed to follow that of a general planar antenna

$$G(\gamma,\lambda) = G_0 \mathrm{sinc}^2\left(\frac{A\pi}{\lambda_0}\sin\gamma\cos\lambda\right)\mathrm{sinc}^2\left(\frac{B\pi}{\lambda_0}\sin\gamma\sin\lambda\right) \tag{8}$$

where G_0 is the maximum gain and A and B are the antenna dimensions in the along and across directions, respectively.

III. Simulation of ASIRAS Echoes

In the following, we discuss the calculation of surface and volume echoes for various snow-covered sea ice types. The total echo is the sum of surface and volume echoes according to the first-order radiative transfer solution (see, e.g., [10]). Calculations are simplified by ignoring the effects of aircraft attitude errors, radar speckle, and noise. Thus, the simulated echoes represent averages of the measured ones.

A. Surface Echoes for SLI

Smooth level ice (SLI) is here a level ice type which is unaffected by deformation. The small-scale surface rms height σ of SLI is typically within the validity limits of the IEM single scattering model [11]. The simulation of the snow and ice surface echoes for SLI starts with the calculation of the flat-surface impulse response [4]

$$P_{\rm fs}(\tau) = \frac{\lambda_0^2 P_T}{(4\pi)^3}\left(\frac{1}{2}c_0 H\right)\frac{2}{R^4(\tau)}\int_0^\pi G^2(\gamma,\lambda)d(x)d\lambda \tag{9}$$

where R is the measurement range. The altitude H is that of ASIRAS above the ocean. There is no need to calculate $P_{\rm fs}(\tau)$ separately for snow and sea ice surfaces as their distance difference to the ocean is so small. Now, it is also possible to form a database of the impulse responses at various altitudes for fast calculation of the multilooked echoes.

Next, the following steps are taken: 1) impulse responses are multiplied with the surface backscattering coefficient (σ°) as a function of τ; 2) convolution of this product with the system impulse response $p(t)$ consisting of the main lobe and the first sidelobes; 3) convolution with the surface-roughness probability density function (pdf) $f_{\rm sr}(\tau)$ assumed to be Gaussian; 4) slant-range correction of the echoes; 5) summation of the echoes without weighting to form multilooked echoes for snow and ice surfaces; and 6) time corrections to the multilooked echoes due to the ice freeboard, snow thickness, and slower speed of electromagnetic field in the snow medium. Before slant-range correction, the backscattered echo power as a function of γ can be calculated. The steps 1)–3) can be formulated as

$$P_s(\tau) = f_{\rm sr}(\tau) * p(\tau) * (P_{\rm fs}(\tau)\cdot\sigma^\circ(\tau)) \tag{10}$$

where

$$f_{\rm sr}(\tau) = \frac{1}{\sqrt{2\pi}(2\sigma/c_0)}\exp\left(-\frac{\tau^2}{2(2\sigma/c_0)^2}\right). \tag{11}$$

Surface σ° is calculated here using the single scattering IEM model for surfaces with small to moderate σ [11]. The single scattering IEM model is valid when $k\sigma < 2$ [10]; at 13.5 GHz, this means that $\sigma < 0.71$ cm. A coherent backscattering model has been presented in [12]. The coherent model accounts for the sphericity of the wavefront, small-scale σ, and $p(t)$. It was derived using a Gaussian antenna beam, and it is valid for a traditional pulsewidth-limited altimeter. In the case of a beamforming altimeter like ASIRAS, its validity needs further considerations.

Authorized licensed use limited to: Danmarks Tekniske Informationscenter. Downloaded on November 25, 2009 at 07:27 from IEEE Xplore. Restrictions apply.

The effect of the snow medium to sea ice σ° is obtained by

$$\sigma^\circ = T_s^2(0^\circ)\exp(-2\kappa_{\rm es}h_s)\sigma^\circ(\text{bare sea ice}) \qquad (12)$$

where T_s is the power transmission coefficient of the snow surface, $\kappa_{\rm es}$ is the volume extinction coefficient of snow, and h_s is snow thickness.

B. Surface Echoes for RLI and DI

Rough level ice (RLI) is an ice type which has protruding ice blocks and floe edges and low uneven surface areas, and it has typically broken and frozen several times. DI consists of, for example, ice ridges, brash ice, and RLI areas with highly variable area fractions.

Here, as a first approximation, the simulation of echoes for RLI and DI is carried out using ice freeboard pdfs derived from the ALS data [13]. These pdfs were calculated for windows of 200 m by 200 m with a resolution of 2 cm. The ice surface is assumed to consist of small horizontal ice facets at different elevations whose occurrence density is determined with the ice freeboard pdf. The ice facets have superimposed small-scale σ, and it is assumed that only incoherent scattering occurs (i.e., no specular reflections from the facets) which is quantified with the IEM model. Multilooked echoes are calculated as for the snow-covered SLI. The resolution of the ice freeboard pdfs is interpolated to that used in the echo calculations. The interpolated pdfs are moved in time so that their means are at zero while the original measured mean ice freeboards are used for the time correction of the multilooked echoes.

C. Volume Echoes

Snow and ice volume multilooked echoes are obtained starting with a distribution function $v(\tau)$, which describes the volume scattering cross-section per unit volume as a function of depth when only the two-way vertical path within the volume needs to be considered [4]. For homogenous medium, $v(\tau)$ is given as

$$v(\tau) = \frac{1}{2}T^2(0)\kappa_s c\exp(-\kappa_e c\tau), \qquad \tau > 0, \quad \tau < 2h/c \qquad (13)$$

where κ_s and κ_e are volume scattering and extinction coefficients, respectively, c is the wave speed in the medium, and h is the medium thickness. For layered snow and ice media, the total $v(\tau)$ is obtained by taking into account attenuations of different layers and ignoring reflections between layers of same medium. Next, the total $v(\tau)$ is convolved with the flat-surface impulse responses, and then, steps 2)–6) in Section III-A are carried out.

Another way is to start from the calculation of volume impulse responses, which require integration over γ and λ [14]. However, their calculation is very time-consuming. In addition, the differences between these two methods for homogeneous media were small. Snow and sea ice κ_s's are obtained from the Rayleigh scattering theory with spherical ice crystals in snow and spherical air bubbles in sea ice [10]. κ_e is a sum of κ_s and volume absorption coefficient κ_a based on the effective dielectric constants [15]–[18].

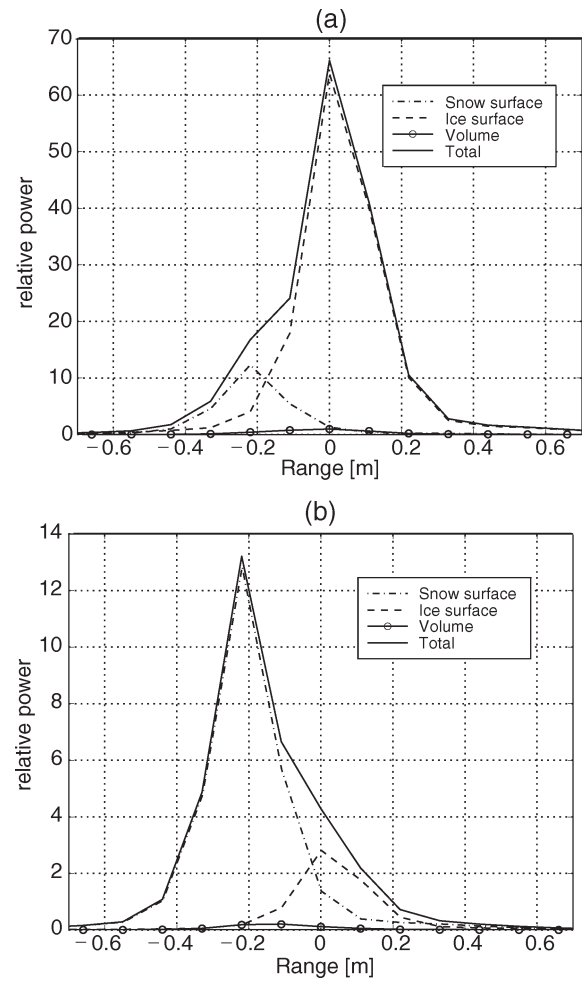

Fig. 1. ASIRAS echoes for SLI covered with (a) dry snow and (b) moist snow (volumetric wetness 1%). Snow thickness is 20 cm. Freeboard is 4.1 cm. Range 0 m corresponds to an altitude of 300 m.

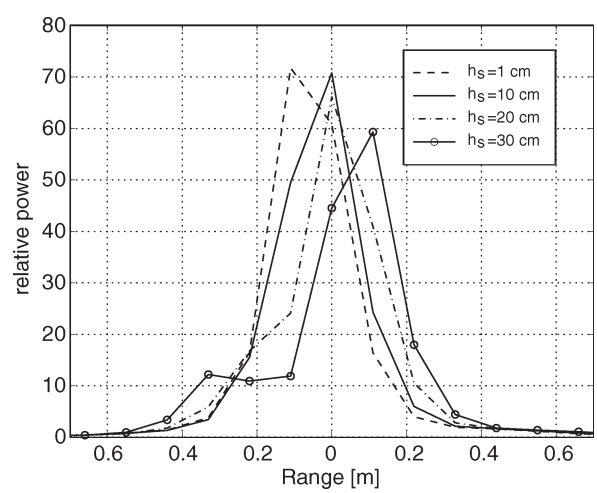

Fig. 2. ASIRAS total echo for SLI as a function of snow thickness. Snow cover is dry. Range 0 m corresponds to an altitude of 300 m.

D. Time Resolution in Simulations

All calculations are carried out using a time resolution $s_p/100$ which is around 90 times better than the ASIRAS resolution of 0.73 ns, and both the total echo and individual

Authorized licensed use limited to: Danmarks Tekniske Informationscenter. Downloaded on November 25, 2009 at 07:27 from IEEE Xplore. Restrictions apply.

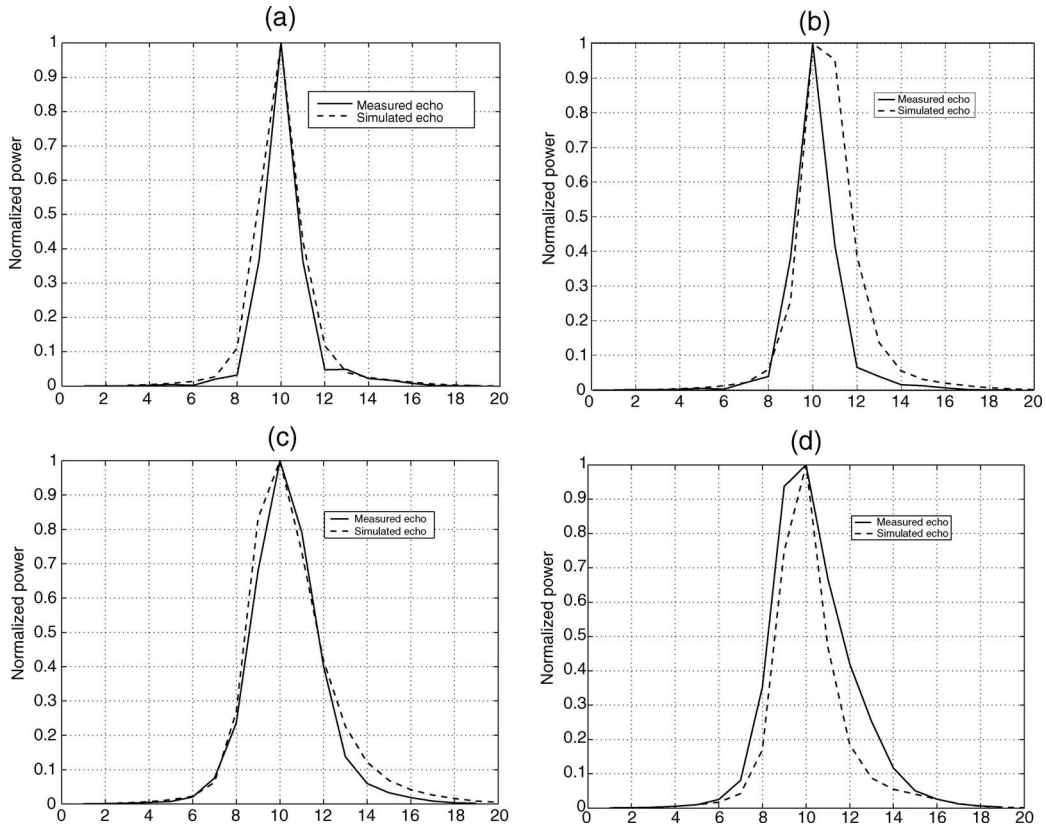

Fig. 3. Simulated and measured mean ASIRAS echoes [(a) and (b)] for RLI and [(c) and (d)] for DI. (a) and (c) are examples of good match between the echoes, and (b) and (d) are examples of the poor match. Mean ice freeboards are 3.1, 6.3, 19.6, and 12.9 cm in (a), (b), (c), and (d), respectively. Altitude is 300 m.

snow and ice echoes are integrated to the ASIRAS resolution in the end.

IV. Simulation Results

In the following, the effects of various parameters to the simulated ASIRAS echoes for SLI are first discussed, and then, simulated and measured echoes are briefly compared to each other. The following basic values for the snow and sea ice media are used: snow density $\rho_s = 0.25$ g/cm^3, snow volumetric wetness $W = 0\%$, snow temperature $T_s = -5$ °C, ice crystal diameter $d_s = 1$ mm, snow surface roughness $\sigma_s = 0.2$ cm, snow surface correlation length $L_s = 2$ cm, ice thickness $h_i = 60$ cm, ice density $\rho_i = 0.85$ g/cm^3, ice salinity $S = 1\%$, ice temperature $T_i = -1.5$ °C, diameter of air bubbles $d_i = 2$ mm, ice $\sigma_i = 0.2$ cm, ice $L_i = 2$ cm, and exponential autocorrelation function for both snow and ice surfaces. These values are based on the CryoVex 2005 field campaign data and ground truth data measured in the Bay of Bothnia in [19]. An altitude of 300 m is used in the simulations.

A. Effect of Snow Wetness and Thickness

An example of ASIRAS multilooked echoes for SLI covered either with dry or moist $(W = 1\%)$ snow layer (thickness $h_s = 20$ cm) is shown in Fig. 1. Under dry snow conditions, the ice surface echo clearly dominates and the volume echo is negligible. When the 20-cm-thick snow cover becomes moist, the snow surface echo is the largest one, and the power level of the total echo is greatly decreased due to the increased attenuation of snow.

The contribution of the volume echo increases with increasing snow and sea ice albedo. For example, when h_s increases to 30 cm and d_s to 2 mm, the snow volume echo has a noticeable effect on the leading edge of the total echo.

When snow wetness increases, the change of contributions of snow and sea ice surface echoes to the total echo depends greatly on h_s and surface roughness. If snow and ice surfaces have equal roughness (σ and L), the snow surface echo never reaches the power level of the ice surface echo because the dielectric contrast on the snow surface is always much smaller than on the ice surface, even when snow is very wet. Increasing W results in an increase in retrieved ice freeboard.

The effect of variable h_s, from 1 to 30 cm, to the total echo is shown in Fig. 2. The corresponding variation of ice freeboard is from 8.9 to 1.6 cm. When h_s increases, the total echo moves slowly to larger range values and the contribution of the snow cover becomes more visible, but the overall variation of the echo is rather small.

In summary, the simulation results suggest that the accurate estimation of ice freeboard is possible from the ASIRAS data only under dry conditions, and even then, it is a difficult task if the snow load is unknown.

B. Effect of Surface Roughness

The level of σ° with the IEM model is very sensitive to the surface roughness at incidence angles close to 0°, e.g., ice

Authorized licensed use limited to: Danmarks Tekniske Informationscenter. Downloaded on November 25, 2009 at 07:27 from IEEE Xplore. Restrictions apply.

surface σ° is $+1.4$ and -9.2 dB when σ_i is 0.2 and 0.4 cm, respectively (L_i is 2 cm). By varying only slightly the snow and ice σ and L parameters, it is possible to obtain very different surface echo contributions to the total echo. In modeling the ENVISAT altimeter echoes for ice sheets, a high echo sensitivity to small-scale surface roughness has been observed [20]. Consequently, ground truth data on snow and ice surface roughness are needed for more realistic ASIRAS echo simulations.

C. Comparison of Simulated and Measured Echoes

A brief comparison of simulated echoes to those measured in CryoVex 2005 has been conducted. To simplify the echo simulation, the effect of a very thin dry snow cover was ignored. Fig. 3 shows examples of simulated echoes and averages of five measured echoes for RLI and DI. Only a small number of measured echoes can be averaged due to the rapidly varying altitude of the aircraft. In many cases, there was a very good match between the echo shapes for both RLI and DI; however, we include in Fig. 3 examples of worse agreement between the simulations and measurements. The degree of the echo match depends besides on selected scattering and geometric models for sea ice also to some degree on attitude errors of the aircraft and approximations currently used for the ASIRAS beam function and antenna gain.

V. Conclusion

A simulator has been written in Matlab for the calculation of ASIRAS multilooked echoes for snow-covered first-year sea ice. The simulator is a useful tool for understanding the relationships between the snow and ice characteristics and the measured echoes.

The simulation results suggest that when the snow cover is dry, the ice surface echo typically dominates. Accurate estimation of ice freeboard is likely possible only under dry snow conditions and when snow load is known. Simulated echoes are very sensitive to the snow and ice surface roughness. For realistic ASIRAS echo simulation, ground truth data on surface roughness are therefore needed. There was typically a rather good match between the normalized simulated echoes and measured average echoes. However, this match depends on the selected scattering and geometric models for the sea ice, and further studies with other models are needed before we can quantify how accurately the ASIRAS simulator can model measured echoes.

Topics for further research include a more realistic scattering model for both level ice and DI which includes also coherent scattering, and more realistic parameterization of layered snow and sea ice media.

The ASIRAS simulator concept can also be used for the CryoSat altimeter. Needed CryoSat characteristics can be found in [2].

References

[1] C. Mavrocordatos, E. Attema, and M. Davidson, "Development of ASIRAS (Airborne SAR/Interferometric Altimeter System)," in *Proc. IGARSS*, 2004, pp. 2465–2467.

[2] D. J. Wingham, C. R. Francis, S. Baker, C. Bouzinac, D. Brockley, R. Cullen, P. deChateau-Thierry, S. W. Laxon, U. Mallow, C. Mavrocordatos, L. Phalippou, G. Ratier, L. Rey, F. Rostan, P. Viau, and D. W. Wallis, "CryoSat: A mission to determine the fluctuations in Earth's land and marine ice fields," *Adv. Space Res.*, vol. 37, no. 4, pp. 841–871, 2006.

[3] V. Helm, S. Hendricks, S. Goebell, W. Rack, C. Haas, U. Nixdorf, and T. Boebel, "CryoVex 2004 and 2005 (BoB) data acquisition and final report," Alfred Wegener Inst., Bremerhaven, Germany, 2006. ESA Contract C18677/04/NL/GS.

[4] D. J. Wingham, L. Phalippou, C. Mavrocordatos, and D. Wallis, "The mean echo and echo cross product from a beamforming interferometric altimeter and their application to elevation measurement," *IEEE Trans. Geosci. Remote Sens.*, vol. 42, no. 10, pp. 2305–2323, Oct. 2004.

[5] R. Tonboe, S. Andersen, and L. T. Pedersen, "Simulation of the Ku-band radar altimeter sea ice effective scattering surface," *IEEE Geosci. Remote Sens. Lett.*, vol. 3, no. 2, pp. 237–240, Apr. 2006.

[6] K. A. Giles, S. W. Laxon, D. J. Wingham, D. W. Wallis, W. B. Krabill, C. J. Leuschen, D. McAdoo, S. S. Manizade, and R. K. Raney, "Combined airborne laser and radar altimeter measurements over the Fram Strait in May 2002," *Remote Sens. Environ.*, vol. 111, no. 2/3, pp. 182–194, Nov. 2007.

[7] R. Cullen, ESA, ESTEC, Jun. 2007. private communication.

[8] R. Cullen, "ASIRAS product description," ESA/ESTEC, Noordwijk, The Netherlands, Rep. CS-LI-ESA-GS-0371, 2006. issue 2.3.

[9] C. Fischer and M. Younis, "Planar antenna arrays for an experimental altimeter ASIRAS," Institut für Höchstfrequenztechnik und Elektronik, Univ. Karlsruhe, Karlsruhe, Germany, Rep. ASIRAS-RST-TR-0002, 2004.

[10] A. K. Fung, *Microwave Scattering and Emission Models and Their Applications*. Norwood, MA: Artech House, 1994.

[11] A. K. Fung, Z. Li, and K. S. Chen, "Backscattering from a randomly rough dielectric surface," *IEEE Trans. Geosci. Remote Sens.*, vol. 30, no. 2, pp. 356–369, Mar. 1992.

[12] A. K. Fung and H. J. Eom, "Coherent scattering of a spherical wave from an irregular surface," *IEEE Trans. Antennas Propag.*, vol. AP-31, no. 1, pp. 68–72, Jan. 1983.

[13] M. Similä, M. Mäkynen, I. Heiler, and M. Hallikainen, "Comparison between ENVISAT SAR and 3-D laser scanner statistics for the Baltic Sea Ice," in *Proc. IGARSS*, Boston, MA, 2008.

[14] M. H. Newkirk and G. S. Brown, "A waveform model for surface and volume scattering from ice and snow," *IEEE Trans. Geosci. Remote Sens.*, vol. 34, no. 2, pp. 444–456, Mar. 1996.

[15] M. Hallikainen, F. T. Ulaby, and M. Abdelrazik, "Dielectric properties of snow in the 3 to 37 GHz range," *IEEE Trans. Antennas Propag.*, vol. AP-34, no. 11, pp. 1329–1340, Nov. 1986.

[16] M. Tiuri, A. Sihvola, E. Nyfors, and M. Hallikainen, "The complex dielectric constant of snow at microwave frequencies," *IEEE J. Ocean. Eng.*, vol. OE-9, no. 5, pp. 377–382, May 1984.

[17] M. Hallikainen and D. P. Winebrenner, "The physical basis for sea ice remote sensing," in *Microwave Remote Sensing of Sea Ice*, F. Carsey, Ed. Washington, DC: AGU, 1992, pp. 28–46.

[18] G. F. N. Cox and W. F. Weeks, "Equations for determining the gas and brine volumes in sea ice samples," *J. Glaciol.*, vol. 29, no. 102, pp. 306–316, 1983.

[19] A. Carlström and L. M. H. Ulander, "Validation of backscatter models for level and deformed ice sea ice in ERS-1 SAR images," *Int. J. Remote Sens.*, vol. 16, no. 7, pp. 3245–3266, 1995.

[20] P. Lacroix, M. Dechambre, B. Legrésy, F. Blarel, and F. Rémy, "On the use of the dual-frequency ENVISAT altimeter to determine snowpack properties of the Antarctic ice sheet," *Remote Sens. Environ.*, vol. 112, no. 4, pp. 1712–1729, Apr. 2008.

Authorized licensed use limited to: Danmarks Tekniske Informationscenter. Downloaded on November 25, 2009 at 07:27 from IEEE Xplore. Restrictions apply.